Spectral Methods for the Euler Equations: The Blunt Body Problem Revisited

David A. Kopriva*
Florida State University, Tallahassee, Florida 32306
and
Thomas A. Zang† and M. Yousuff Hussaini‡
NASA Langley Research Center, Hampton, Virginia 23665

We solve the blunt body problem using shock fitting and a Chebyshev spectral collocation method. Careful attention is paid to the boundary and shock acceleration equations. We show that converged solutions can be obtained without artificial smoothing and that spectral accuracy is observed.

Introduction

FLOW stability problems require accurate mean flow solutions. For these problems spectral methods promise to be more accurate for a given number of grid points than the more commonly used finite difference methods. First, the error decays exponentially fast for smooth enough solutions.[1] Often, the addition of a single grid point can decrease the error by an order of magnitude. The low inherent dissipation of spectral methods means that the computed solutions are not excessively smoothed and that artificial viscous effects are not observed. Finally, information is defined globally. It is thus possible to interpolate accurately the computed solution onto any particular grid that may be required by a stability analysis code.

Spectral solutions to the blunt body problem have appeared in Hussaini et al.[2] and Yasuhara et al.[3] Both papers fit the bow shock so that the solution was smooth in the computed region. The first paper considered inviscid two-dimensional flow over a right circular cylinder for freestream conditions with and without shear. It showed that features in the solution could be represented on very coarse meshes when the spectral technique was used. The second paper considered inviscid and viscous flows for more complicated bodies in both two and three dimensions and compared some results to experimental data.

Though the spectral method gave good qualitative and quantitative results, two difficulties were noted in Ref. 2. First, the solutions developed spurious oscillations that were removed by the application of artificial smoothing. Also, a low Courant number (based on the smallest grid spacing) of 0.2 appeared necessary to maintain numerical stability. Such artificial smoothing is undesirable for spectral methods: it adds significantly to the overall cost of the solution, it reduces the overall accuracy, and it eliminates high-frequency information, thereby acting effectively as an unwanted artificial viscosity.

The second problem with the spectral calculations that have been presented to date is that fully converged steady-state solutions were not obtained. Hussaini et al.[2] comment that the stagnation pressure in their calculations after 2000 time steps on a 9×9 grid was converged to only three or four decimal places. Yasuhara et al.[3] did not demonstrate satisfactory convergence to the steady state.

In this paper, we present improved boundary and shock conditions that not only do not require artificial smoothing to obtain nonoscillatory solutions to the inviscid blunt body problem but also produce converged steady-state solutions. Finally, we show that the accuracy is spectral.

Blunt Body Problem

A schematic of the problem we consider is shown in Fig. 1. A blunt body of radius $r_b(\theta)$ is placed in a freestream having Mach number $M > 1$. A shock wave of radius $r_s(\theta,t)$ forms about the body. In the absence of viscous effects, the Euler equations of gasdynamics describe the smooth part of the flow between the shock and the body. (See Ref. 2 for details.)

Four types of boundaries to the flow are present. The body itself corresponds to a streamline so the normal velocity is zero. The streamline at $\theta = \pi$ is a symmetry axis so the normal velocity and the θ derivatives of the pressure, entropy, and radial velocities are zero. The shock wave is treated explicitly as a boundary of the flow, with upstream conditions prescribed. The final boundary is placed at $\theta = \theta_{\max}$ beyond the sonic line so that the flow exits at supersonic speed and no explicit boundary conditions are necessary.

For the purposes of the computation, the region between the shock and the body is mapped onto the unit square by the transformations

$$X = \frac{r - r_b(\theta)}{r_s(\theta,t) - r_b(\theta)} \tag{1a}$$

$$Y = \frac{\pi - \theta}{\pi - \theta_{\max}} \tag{1b}$$

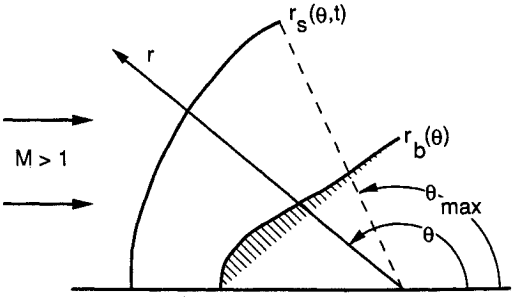

Fig. 1 Geometry of the blunt body problem.

Received Nov. 13, 1989; revision received July 6, 1990.

*Associate Professor, Department of Mathematics and Supercomputer Computations Research Institute. Member AIAA.
†Research Scientist, Theoretical Flow Physics Branch, Fluid Mechanics Division, MS 156. Member AIAA.
‡Chief Scientist, Institute for Computer Applications in Science and Engineering, MS 132C. Associate Fellow AIAA.

In this new (time-dependent) coordinate system, the equations to be solved are

$$P_t + UP_X + VP_Y + \gamma\{X_r u_X + (X_\theta/r)v_X + (Y_\theta/r)v_Y + u/r + \xi[u/r + v\cot(\theta)/r]\} = 0$$

$$u_t + Uu_X + Vu_Y + (a^2/\gamma)X_r P_X - v^2/r = 0$$

$$v_t + Uv_X + Vv_Y + (a^2/\gamma r)(X_\theta P_X + Y_\theta P_Y) + uv/r = 0$$

$$s_t + Us_X + Vs_Y = 0 \tag{2}$$

where the contravariant velocity components are

$$U = X_t + uX_r + (v/r)X_\theta$$

$$V = (v/r)Y_\theta$$

and where P is the logarithm of the pressure, u the radial velocity, v the angular velocity, and s the entropy. The sound speed is $a = \sqrt{\gamma}\exp\{[(\gamma-1)P - s]/2\gamma\}$ where $\gamma = 1.4$. The parameter ξ is zero for two-dimensional flow and one for axisymmetric flow. The flow variables are normalized to their freestream values at upstream infinity so that $P_\infty = s_\infty = 0$ and $a_\infty^2 = \gamma$.

Spectral Solution

Details on Chebyshev spectral methods can be found in Ref. 1. For this problem, the interior points are discretized as described in Ref. 2. The only modification is that a midpoint rule (sometimes known as the modified Euler method) is used to integrate the equations in time. The significant changes to the code of Ref. 2 have been made to the boundary and shock equations.

Along the body, only one boundary condition, that of zero normal velocity, is allowed, so the tangential velocity, entropy, and pressure must be computed. Since the entropy is advected along streamlines, it is computed along the body exactly as it is in the interior. The pressure is computed with a characteristic condition derived as follows: In polar coordinates, the pressure and momentum equations are written as

$$P_t + uP_r + (v/r)P_\theta + R_p = 0$$

$$u_t + (a^2/\gamma)P_r + R_u = 0$$

$$v_t + (a^2/\gamma r)P_\theta + R_v = 0 \tag{3}$$

where

$$R_p = \gamma\{u_r + v_\theta/r + u/r + \xi[u/r + v\cot(\theta)/r]\}$$

$$R_u = uu_r + (v/r)u_\theta - v^2/r$$

$$R_v = uv_r + (v/r)v_\theta - uv/r$$

These are combined as

$$[P_t + uP_r + (v/r)P_\theta + R_p] \pm (\gamma/a)[N_1(u_t + (a^2/\gamma)P_r + R_u) + N_2(v_t + (a^2/\gamma r)P_\theta + R_v)] = 0 \tag{4}$$

where $N = (N_1, N_2)$ is the normal vector to the body. The wall boundary condition implies that $N_1 u + N_2 v = 0$ for all time, so the time derivative terms on u and v vanish in Eq. (4). If the tangential velocity is defined as $V = N_2 u - N_1 v \equiv \boldsymbol{T}\cdot\boldsymbol{q}$, where $\boldsymbol{q}$ is the velocity, Eq. (4) can be rewritten as the differential equation

$$P_t = -[\pm a\,\nabla P\cdot N + V\,\nabla P\cdot T + R_p \pm (\gamma/a)(N_1 R_u + N_2 R_v)] \tag{5}$$

(The lower sign is appropriate when the normal is defined to point into the domain.) To approximate Eq. (5), we replace the spatial derivatives

$$\frac{\partial}{\partial r} = X_r\frac{\partial}{\partial X} + Y_r\frac{\partial}{\partial Y}$$

$$\frac{\partial}{\partial \theta} = X_\theta\frac{\partial}{\partial X} + Y_\theta\frac{\partial}{\partial Y}$$

by the spectral approximations computed at the boundary, and the equation is integrated in time just as the interior points are integrated.

The tangential velocity is computed from the tangential momentum equation obtained by combining the second and third of Eq. (3); i.e.,

$$V_t = (\boldsymbol{T}\cdot\boldsymbol{q})_t = -(a^2/\gamma)(N_1 P_r + N_2 P_\theta) - (N_1 R_u + N_2 R_v) \tag{6}$$

This equation, together with the normal velocity condition $N\cdot q = 0$, suffices to specify completely the velocity components u and v at each time level.

The boundary condition at $\theta = \pi$ is enforced by setting $v = 0$. Symmetry is enforced by replacing the computed derivatives P_Y, s_Y, and u_Y at the boundary by zero.

The most complicated boundary is the shock boundary corresponding to $X = 1$. The procedure is basically that described by Moretti[4] extended to two dimensions. Let variables with subscript 1 denote values on the low-pressure (upstream, specified flow) side of the shock and subscript 2 denote values on the high-pressure (unknown) side. With all unknowns scaled to the values at upstream infinity, the Rankine-Hugoniot relations that describe the pressure and normal velocity jumps across the shock are

$$P_2 = P_1 + \ell n\left[\delta_1^2 - \frac{\gamma-1}{2}\right] - \ell n\left(\frac{\gamma+1}{2}\right)$$

$$\delta_2 = \frac{\gamma-1}{\gamma+1}\delta_1 + \frac{2\gamma}{\gamma+1}\frac{1}{\delta_1} \tag{7}$$

where $\delta_i = \boldsymbol{q}_i\cdot N - wN_1$ is the normal velocity relative to the shock, and $w = \partial r_s/\partial t$ is the shock speed. Under the assumption that the flow upstream of the shock is stationary in time, Eq. (7) is differentiated with respect to time to give

$$\dot{P}_2 = G\dot{\delta}_1, \qquad \dot{\delta}_2 = F\dot{\delta}_1 \tag{8}$$

where the coefficients F and G depend only on quantities on the low-pressure (prescribed) side:

$$F = \frac{\gamma-1}{\gamma+1} - \frac{2\gamma}{(\gamma+1)\delta_1^2}$$

$$G = \frac{2\delta_1}{[\delta_1^2 - (\gamma-1)/2]}$$

Equations (8) for $\dot{P}_2$ and $\dot{\delta}_2$ are substituted into the compatibility equation [cf. Eq. (4)]

$$[P_t + uP_r + (v/r)P_\theta + R_p] - (\gamma/a)\{N_1[u_t + (a^2/\gamma)P_r + R_u] + N_2[v_t + (a^2/\gamma r)P_\theta + R_v]\} = 0 \tag{9}$$

which describes waves propagating into the shock from the downstream side, again for the inward pointing normal. The resulting equation is solved for the shock acceleration:

$$\dot{w} = \frac{\boldsymbol{q}_1\cdot\dot{N}(aG - \gamma F) - w\dot{N}_1(aG - \gamma F + \gamma) + \gamma\boldsymbol{q}_2\cdot\dot{N} + aC}{N_1(aG - \gamma F + \gamma)} \tag{10}$$

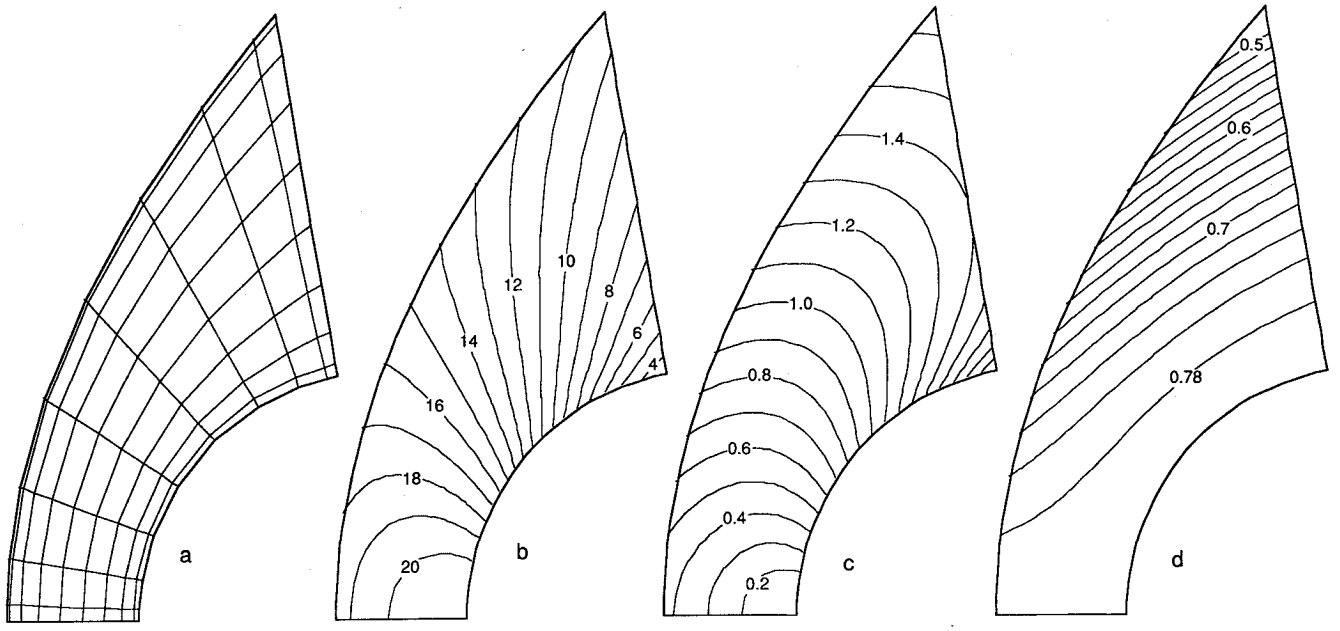

Fig. 2 Grid and contours of the spectral solutions to the $M = 4$ uniform flow over a circular cylinder: a) grid, b) pressure, c) Mach number, and d) entropy.

The quantities on the right can all be determined from derivatives of the flow variables in the computational domain and of the shock speed. First,

$$C = (q_1 - aN) \cdot \nabla P + R_p - (\gamma/a)(N_1 R_u + N_2 R_v)$$

The time derivatives of the shock normal are related to the shock speed. The shock normals are

$$N_1 = -(1/R), \qquad N_2 = Q/R$$

where

$$R = \sqrt{1 + Q^2}, \qquad Q = \frac{1}{r_s}\frac{\partial r_s}{\partial \theta}$$

Then the time derivatives can be written as

$$\dot{N}_1 = \frac{Q}{r_s R^3}\left(\frac{\partial w}{\partial \theta} - wQ\right)$$

$$\dot{N}_2 = \dot{N}_1 / Q$$

The θ derivative of the shock speed is computed spectrally.

A simpler, alternative procedure for shock fitting has been described in Ref. 1. This procedure uses the first part of Eq. (8) and P_t computed from Eq. (2) in the interior to calculate the shock speed. Thus, it does not use a characteristic compatibility relation to calculate the waves which intersect the shock from downstream. Rather, it uses the original differential equation, which includes the contribution of both upstream and downstream moving waves. If we substitute for $\dot{\delta}_1$ in Eq. (8), and solve for $\dot{w}$,

$$\dot{w} = \frac{G(q_1 \cdot \dot{N} - w\dot{N}_1) - \dot{P}_2}{GN_1} \tag{11}$$

Results

We have successfully computed the solutions for uniform flow over a circular cylinder and other two-dimensional and axisymmetric geometries in the Mach number range of 2–25 using the characteristic boundary conditions and full characteristic shock acceleration formula [Eq. (10)]. In no case was filtering required. As examples, we report the $M = 4$ case for two-dimensional flow over a circular cylinder and axisymmetric flow over a blunt nosed cone. By our examples, we seek to show that convergent, spectrally accurate solutions are possible without the need for added artificial smoothing.

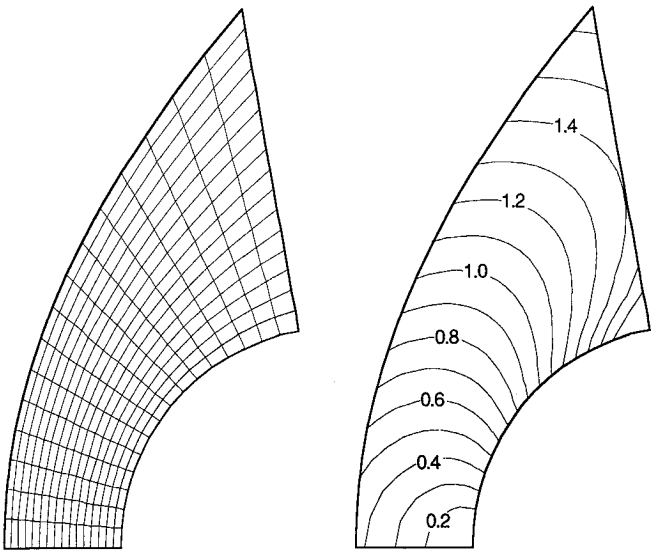

Fig. 3 Grid and Mach number contours of the MacCormack solution corresponding to the case in Fig. 2.

Figure 2 shows the pressure, Mach number, and entropy contours with the 10×10 point grid on which they were computed for the spectral solution of the flow over a circular cylinder. The outflow boundary angle θ_{max} was 80 deg, and the solution was computed with a CFL number of 0.9, based on the smallest grid spacing and the largest wave speed. To avoid the problems associated with contouring on a very coarse grid, all the spectral contour plots have been "expanded" by interpolating the computed results to a fine grid before plotting. For comparison purposes, Fig. 3 shows the Mach contours computed by a MacCormack finite difference scheme, which also used a fitted shock, on a 16×16 point grid. Figures 2c and 3 are qualitatively the same, and like the finite difference results, there are no high-frequency oscillations in the spectral solution.

A slightly more complicated example is the $M = 4$ axisymmetric flow over a blunt cone. A 10×15 point mesh was used

about a body defined by a sphere followed by a 40-deg axisymmetric cone. The outflow boundary was chosen at $\theta_{max} = 90$ deg. The grid, pressure, Mach number, and entropy are plotted in Fig. 4. We used 2500 iterations to compute this solution at a Courant number (based on the finest grid spacing) of 0.9. The solution was converged to 32-bit precision after roughly 1000 iterations. This problem has a slope discontinuity in the body shape where the cone intersects the sphere yet the solution remains smooth.

The spectral solutions converge to steady state. Figure 5a is a plot of the logarithm of the maximum pressure residual for the solutions in Fig. 2 computed to 64-bit precision. By 4500 iterations, the pressure residual has converged to machine zero. This is to be contrasted with the results of Hussaini et al.[2] who did not use characteristic boundary conditions and periodically smoothed the solutions. In their calculations, the residual was still larger than 10^{-4} by 2000 iterations. As a final convergence test, we show in Fig. 5b that the shock velocity also converges to machine zero.

We were not successful using the simplified shock fitting procedure, Eq. (11), without artificial smoothing even though the technique works acceptably with the finite difference approximation. The reason is that spectral methods are more sensitive to boundary conditions than are finite difference methods.[1] Oscillations that are damped by internal dissipation of the finite difference scheme persist and eventually grow in the spectral approximation because its internal dissipation is small. The previously reported calculations in Ref. 2 were successful because oscillations were artificially filtered during the course of the computations. Figure 6 compares the pressure residual history for the two methods, Eqs. (10) and (11), for solutions computed in 32-bit precision. By roughly 1200 iterations, the solution using Eq. (10) has converged to machine precision. Using the simplified formula, the solution diverges after roughly 300 iterations. For early times, when the shock speeds are large, there is little difference between the two solutions. But as the solution nears steady state, the simplified procedure does not accurately predict the shock speed, the result being that oscillations in the pressure and normal velocity build up at the shock.

Spectral accuracy is also now observed. One quantity for which the exact value is known is the stagnation pressure. Figure 7 shows the relative error in the stagnation pressure for the $M = 4$ freestream as a function of the total number of grid points. The present results are compared with the error reported in Ref. 2 and a MacCormack solution. The present spectral results are clearly more accurate than either. The straight line in this semilog plot indicates that the error decays exponentially fast, consistent with other spectral calculations of compressible flows.[1]

We have also compared the cost of the spectral calculations with the cost of the finite difference solutions. For a given number of grid points, the spectral approximation is more

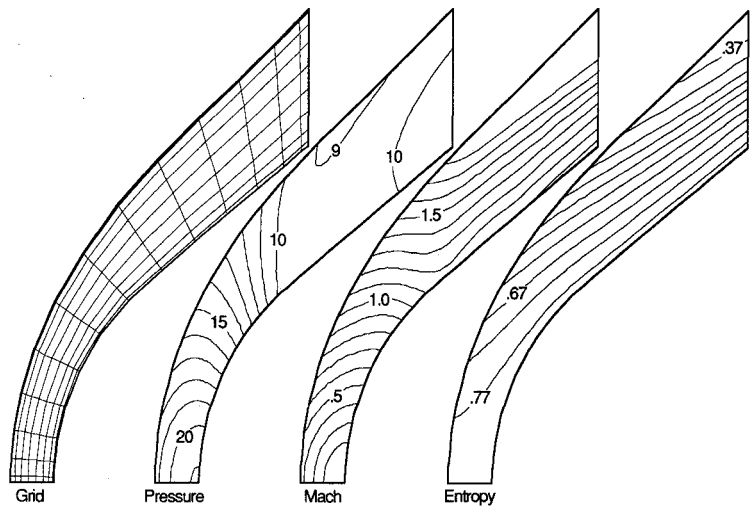

Fig. 4 Grid and flow variables for the spectral solution of uniform $M = 4$ flow over a blunt nose cone.

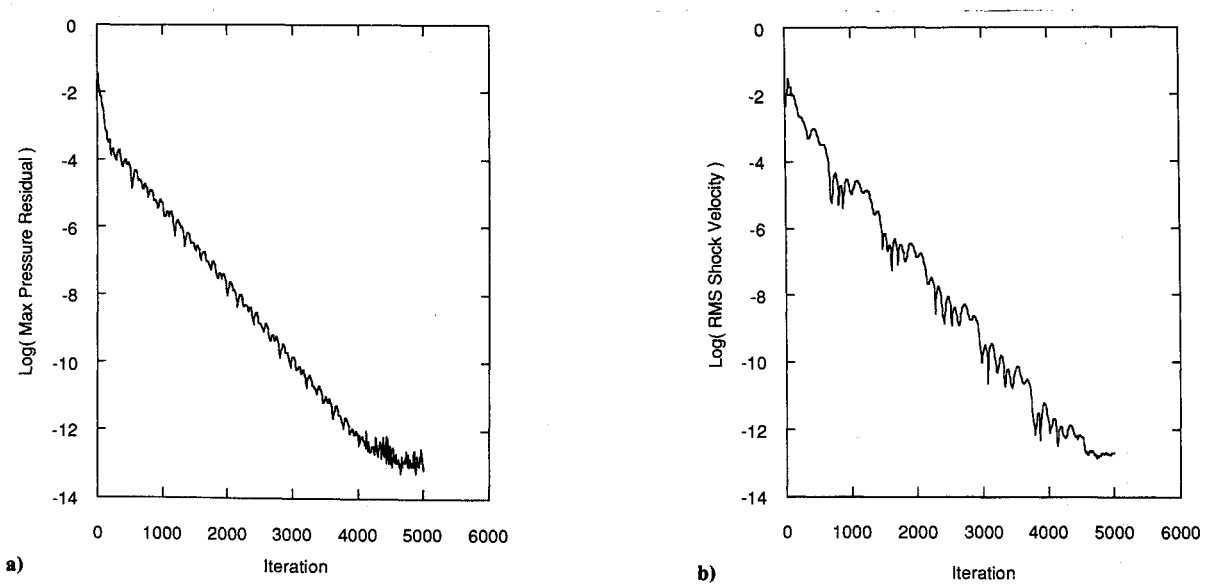

Fig. 5 Convergence histories of the flow in Fig. 2: a) pressure residual, b) shock velocity.

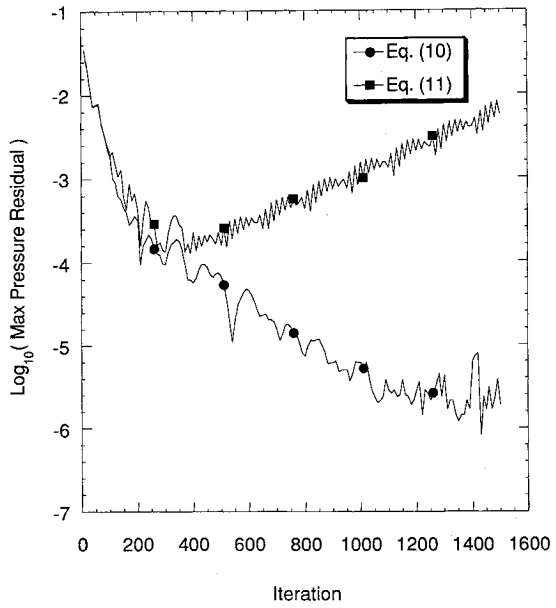

Fig. 6 Comparison of the pressure residual for two shock acceleration formulas.

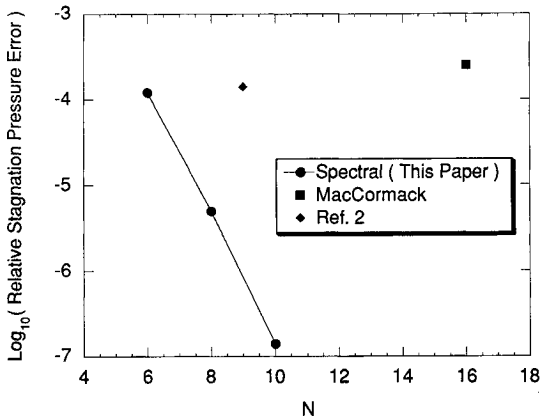

Fig. 7 Relative error in the stagnation pressure vs the number of grid points in each direction.

costly than the finite difference one. First, the calculation of the spectral derivatives (which is typically half of the total calculation time) involves multiplication of the solution vector made up of points along a grid line by a full matrix. The work is $\mathcal{O}(JN^2+NJ^2)$, where N is the number of grid points in the X direction and J is the number in the Y direction. Furthermore, once the spatial part of the equations is discretized spectrally, the resulting system of ordinary differential equations is stiff. Unlike the Courant condition, which governs the time step for the finite difference calculation, the maximum time step that can be taken with the spectral method is proportional to N^{-2} and J^{-2}.

If one compares the work required for a given accuracy, the spectral method is more competitive. For the blunt body programs used here, neither of which were hand optimized, the spectral method is more efficient. As an example, we again consider the $M = 4$ flow over the right circular cylinder. Figure 8 compares the convergence of a 6×6 point spectral solution and a 21×21 point finite difference solution as a function of the work required measured in CPU time on a Macintosh II (scalar, 32 bit) computer. The relative errors in the stagnation pressure for the spectral and finite difference

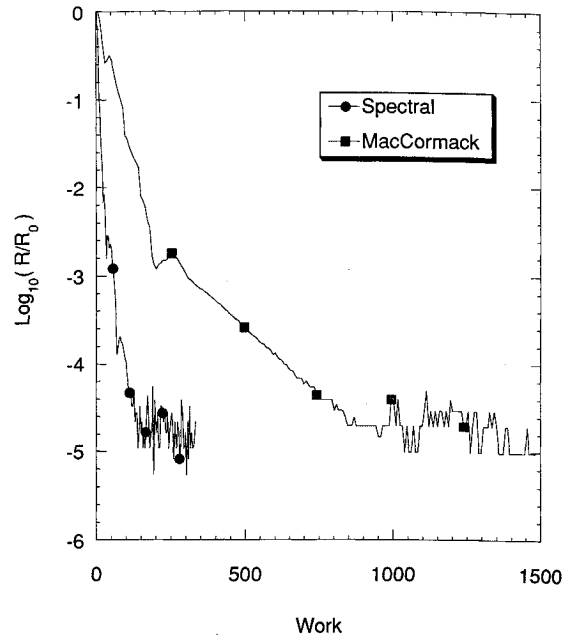

Fig. 8 Comparison of the work required to reach steady state at comparable accuracy for spectral and finite difference solutions of the $M = 4$ flow over a circular cylinder. Plotted are the residuals normalized to the initial residual vs the work.

solutions are 1.24×10^{-4} and 1.5×10^{-4}, respectively. For this problem, which has relatively little structure in the solution, the finite difference code requires over six times the work of the spectral code to reach steady state.

Conclusions

We have described boundary and shock fitting procedures with which spectrally accurate solutions to the blunt body problem can be computed without the need for artificial smoothing. The essence of these procedures is the use of characteristic compatibility relations to compute the body pressure and shock velocity.

Acknowledgment

This research was supported in part by NASA under Contract NAG1-862 and by the U.S. Department of Energy through Contract DE-FC05-85ER250000 (first author); and by NASA Contract NAS1-18605 while the third author was in residence at the Institute for Computer Applications in Science and Engineering, NASA Langley Research Center. We thank M. D. Salas for the use of his MacCormack blunt body code on which the spectral code is based.

References

[1]Canuto, C., Hussaini, M. Y., Quarteroni, A., and Zang, T. A., *Spectral Methods in Fluid Mechanics,* Springer-Verlag, New York, 1987.

[2]Hussaini, M. Y., Kopriva, D. A., Salas, M. D., and Zang, T. A., "Spectral Methods for the Euler Equations: Part II—Chebyshev Methods and Shock-fitting," *AIAA Journal,* Vol. 23, No. 2, 1985, pp. 234–240.

[3]Yasuhara, M., Nakamura,Y., and Wang, J.-P., "Numerical Calculation of Hypersonic Flow by the Spectral Method," *Proceedings of the 11th International Conference on Numerical Methods in Fluid Dynamics,* edited by D. L. Dwoyer, M. Y. Hussaini, and R. G. Voigt, Lecture Notes in Physics, Vol. 323, Springer-Verlag, Berlin, pp. 607–611.

[4]Moretti, G., "Thoughts and Afterthoughts about Shock Computations," Polytechnic Inst. of Brooklyn, New York, PIBAL Rept. 72-37, Dec. 1972.